

Functional Morphology of the Gills of the Shortfin Mako, *Isurus oxyrinchus*, a Lamnid Shark

Nicholas C. Wegner,^{1*} Chugey A. Sepulveda,² Kenneth R. Olson,³ Kelly A. Hyndman,⁴ and Jeffrey B. Graham¹

¹The Center for Marine Biotechnology and Biomedicine, Marine Biology Research Division, Scripps Institution of Oceanography, University of California San Diego, La Jolla, California 92093

²Pfleger Institute of Environmental Research, Oceanside, California 92054

³Indiana University School of Medicine, South Bend Center for Medical Education, University of Notre Dame, Notre Dame, Indiana 46566

⁴Vascular Biology Center, Medical College of Georgia, Augusta, Georgia 30912

ABSTRACT This study examines the functional gill morphology of the shortfin mako, *Isurus oxyrinchus*, to determine the extent to which its gill structure is convergent with that of tunas for specializations required to increase gas exchange and withstand the forceful branchial flow induced by ram ventilation. Mako gill structure is also compared to that of the blue shark, *Prionace glauca*, an epipelagic species with lower metabolic requirements and a reduced dependence on fast, continuous swimming to ventilate the gills. The gill surface area of the mako is about one-half that of a comparably sized tuna, but more than twice that of the blue shark and other nonlamnid shark species. Mako gills are also distinguished from those of other sharks by shorter diffusion distances and a more fully developed diagonal blood-flow pattern through the gill lamellae, which is similar to that found in tunas. Although the mako lacks the filament and lamellar fusions of tunas and other ram-ventilating teleosts, its gill filaments are stiffened by the elasmobranch interbranchial septum, and the lamellae appear to be stabilized by one to two vascular sacs that protrude from the lamellar surface and abut sacs of adjacent lamellae. Vasoactive agents and changes in vascular pressure potentially influence sac size, consequently effecting lamellar rigidity and both the volume and speed of water through the interlamellar channels. However, vascular sacs also occur in the blue shark, and no other structural elements of the mako gill appear specialized for ram ventilation. Rather, the basic elasmobranch gill design and pattern of branchial circulation are both conserved. Despite specializations that increase mako gill area and efficacy relative to other sharks, the basic features of the elasmobranch gill design appear to have limited selection for a larger gill surface area, and this may ultimately constrain mako aerobic performance in comparison to tunas. *J. Morphol.* 000:000–000, 2010. © 2010 Wiley-Liss, Inc.

KEY WORDS: lamnid-tuna convergence; gill surface area; diffusion distance; ram ventilation; interbranchial septum; blue shark

INTRODUCTION

Sharks of the family Lamnidae are convergent with tunas in physiological and morphological

adaptations for fast, continuous swimming and high levels of aerobic performance (review: Bernal et al., 2001). Both lamnids and tunas are streamlined and have undergone comparable changes in myotomal structure in which the red (aerobic) muscle occurs in a more central and anterior position within the body and contributes to the common occurrence of the thunniform swimming mode in both groups (Bernal et al., 2003a; Donley et al., 2004; Shadwick, 2005; Gemballa et al., 2006; Perry et al., 2007). In addition, the blood supply to the red muscle passes through countercurrent heat exchangers (*retia mirabilia*), which conserve aerobic heat produced during continuous swimming (Carey and Teal, 1966; Carey et al., 1971; Bernal et al., 2001). Among the advantages of red-muscle endothermy are increased muscle power output and the acceleration of metabolically mediated processes (Altringham and Block, 1997; Graham and Dickson, 2001; Dickson and Graham, 2004; Bernal et al., 2005). Correspondingly, lamnids and tunas have higher oxygen demands than most other fishes (Brill, 1979, 1987; Graham et al., 1990; Dewar and Graham, 1994; Korsmeyer and Dewar, 2001; Sepulveda et al., 2007) as well as

Contract grant sponsor: National Science Foundation; Contract grant number: IOS-0817774. Contract grant sponsors: Nadine A. and Edward M. Carson Scholarship awarded by the Achievement Rewards for College Scientists (ARCS), Los Angeles Chapter, Tuna Industry Endowment Fund at Scripps Institution of Oceanography, William H. and Mattie Wattis Harris Foundation, Moore Family Foundation, Pfleger Institute of Environmental Research, George T. Pfleger Foundation and the Edna Bailey Sussman Foundation.

*Correspondence to: Nicholas C. Wegner, Scripps Institution of Oceanography, UCSD, 9500 Gilman Dr. Mailcode: 204, La Jolla, CA 92093-0204. E-mail: nwegner@ucsd.edu

Received 4 September 2009; Revised 16 February 2010; Accepted 21 February 2010

Published online in Wiley InterScience (www.interscience.wiley.com)
DOI: 10.1002/jmor.10845

larger hearts with higher cardiac outputs and pressures, elevated blood hemoglobin concentrations and hematocrits, and higher muscle myoglobin concentrations to facilitate oxygen supply to the aerobic musculature (Emery, 1986; Brill and Bushnell, 1991; Bushnell and Jones, 1994; Lai et al., 1997; Bernal et al., 2001; Brill and Bushnell, 2001; Bernal et al., 2003a,b). Despite these convergent characteristics, the overall metabolic capacity of lamnids, while exceeding that of other sharks, does not match that of tunas (Bernal et al., 2003a,b; Sepulveda et al., 2007).

Relatively little is known about comparative aspects of lamnid-tuna convergence of gill structure, which requires modifications for both increased gas transfer to meet high metabolic demands and enhanced gill rigidity to withstand the steady, high-pressure branchial flow induced by ram ventilation. For tunas, gas exchange is enhanced by gill surface areas that are as much as an order of magnitude greater than those of most other teleosts (Muir and Hughes, 1969; Wegner et al., 2010) and by short diffusion distances resulting from slender lamellae with a thin respiratory epithelium (water–blood barrier thickness; Hughes, 1970; Hughes and Morgan, 1973; Hughes, 1984a; Wegner et al., 2006). In addition, a diagonal blood-flow pattern through tuna lamellae minimizes vascular resistance and contributes to gill efficacy by allowing a closer match between the residence time of blood at the exchange surface and the time required for gas transfer (Muir and Brown, 1971; Olson et al., 2003; Wegner et al., 2010). Tuna adaptations for managing the force of the ram-ventilatory stream include lamellar and, in some species, filament fusions that stiffen the gills (Muir and Kendall, 1968; Johnson, 1986; Wegner et al., 2006). In addition, the shape and spacing of tuna lamellae increases gill resistance and helps to slow and streamline branchial flow (Wegner et al., 2010).

Data on lamnid gill structure are limited to two publications on gill surface area. Emery and Szczepanski (1986) found that the gill areas of two lamnids (the shortfin mako, *Isurus oxyrinchus*, $n = 10$ and white shark, *Carcharodon carcharias*, $n = 13$) are 2–3 times greater than those of other pelagic shark species. In contrast, Oikawa and Kanda (1997), who examined only one shortfin mako specimen, reported the gill area to be similar to that of other sharks. Other factors associated with oxygen uptake at the lamnid gill (e.g., lamellar diffusion distances and blood-flow patterns) remain unstudied, and there are no reports describing how lamnid branchial anatomy may be specialized for ram ventilation. Relative to teleosts, the ventilatory flow through elasmobranch gills is more tortuous and involves much greater contact with surfaces that potentially impede flow. Elasmobranchs have interbranchial septa, which originate

at the gill arches, bind adjacent hemibranchs, and extend out to the lateral edge of the body to form the gill flaps. Although this configuration likely stiffens the gills for ram ventilation by binding the trailing edges of the filaments (Benz, 1984), it necessarily imposes greater flow resistance because water passing between the lamellae must subsequently flow through septal channels to exit the branchial chamber.

This study compares the gill structure of the shortfin mako to that of tunas and the blue shark, *Prionace glauca*, a nonlamnid, which, based on its metabolic biochemistry and lack of regional endothermy (Dickson et al., 1993; Bernal et al., 2003b), has lower metabolic requirements. The objective is to determine the extent to which mako gill structure differs from that of other sharks and is convergent with tunas in specializations for increased gas exchange required by heightened aerobic demands and for the continuous force imposed on the gills by fast, continuous swimming.

MATERIALS AND METHODS

Gill Collection

Gills were acquired opportunistically from 20 makos (4.6–71.0 kg, 77.0–187.5 cm FL) and eight blue sharks (2.4–47.8 kg, 72.0–197.0 cm FL) collected for other studies or taken in scientific long-line cruises conducted by the National Marine Fisheries Service in waters off of Southern California and the Hawaiian Islands, USA. Captured sharks were euthanized by severing the spinal cord at the base of the chondrocranium in accordance with protocol S00080 of the University of California, San Diego Institutional Animal Care and Use Committee. The mass of each specimen was determined with an electronic scale or, when direct measurement was not possible (i.e., for seven makos and two blue sharks), by length–weight regression equations (Kohler et al., 1995).

Three procedures were used to prepare the gills for examination:

- 1) For the majority of sharks collected, all five gill arches from one or both sides of the branchial chamber were excised and fixed in 10% formalin buffered in seawater. This tissue was used to determine gill area dimensions, measure lamellar thickness and the water–blood barrier thickness, and examine general morphology using light and scanning electron microscopy (SEM).
- 2) Small sections of the first gill hemibranch were excised from four makos (9.0–33.0 kg, 90.0–132.0 cm FL) and one blue shark (44.0 kg, 197.0 cm FL) and placed in 4% paraformaldehyde in 10 mmol l⁻¹ phosphate-buffered saline (PBS) for 24 h. Fixed tissue was then removed from the paraformaldehyde solution, rinsed in 10 mmol l⁻¹ PBS, followed by two changes of 75% ethanol to remove the fixative. These samples were used in immunochemical treatments to determine the position of mitochondria-rich cells (MRCs) and also to prepare microscope slides for morphological analysis. It is important to note that gill samples prepared in treatments 1 and 2 were excised immediately following euthanasia, and that a low-pressure salt water hose was used to keep the tissues moist during the dissection to prevent the degradation of fine gill structure that occurs with prolonged air exposure following capture (<20 min, Wegner personal observation).
- 3) Five makos (5.0–21.2 kg, 76.0–127.0 cm FL) and two blue sharks (3.4, 17.1 kg; 84.0, 141.0 cm FL) were perfused with microvascular casting solution (either Batson's #17 Anatomical Corrosion Kit, Polysciences, Warrington, PA or Mercocox, Ladd Research, Williston, VT) following the protocol outlined by Wegner et al. (2006). Euthanized sharks were placed ventral side up in a V-shaped cradle, and the gills were irrigated with

aerated sea water. The heart was exposed by midline incision, a catheter inserted, and the specimen was perfused with heparinized shark saline for 2–3 min followed by microvascular casting solution. Perfusions were conducted at 70–95 mmHg, which is consistent with ventral aortic systolic pressures observed in swimming makos (Lai et al., 1997). After complete polymerization (<15 min), the gills were excised from both sides of the branchial chamber; one side was placed in 10% formalin buffered in seawater, and the second was macerated in washes of 10–20% KOH until all of the tissue was removed. The resulting plastic replica casts were then rinsed, air dried, and used for examination of the gill vasculature and for mako gill-area measurements.

Gill Surface Area

Total gill surface area was estimated for five makos (two that had been injected with microvascular casting solution and three that had gill tissue fixed in 10% formalin) following the methods of Muir and Hughes (1969) and Hughes (1984b) and using the equation:

$$A = L_{\text{fil}} \cdot 2n_{\text{lam}} \cdot A_{\text{lam}},$$

where A is total gill surface area, L_{fil} is the total length of all of the gill filaments (i.e., total filament length), n_{lam} is the mean number of lamellae per length of filament (i.e., lamellar frequency; this is multiplied by two to account for the two rows of lamellae, one on each side of the filament), and A_{lam} is the mean bilateral surface area of a lamella.

Total filament length was determined by counting all gill filaments on the five arches from one side of the branchial chamber. Filaments were divided into bins of 20, and the length of each medial filament (i.e., filament number 10, 30, 50, etc.) was measured and assumed to represent the mean filament length for its respective bin (each middle filament was measured from its base, where it is partially covered by a fleshy extension of the gill arch often referred to as the branchial canopy, to the tip). The total length of all the filaments in each bin was calculated, and the bins from all five arches were summed to determine the total filament length for one side of the branchial chamber. This value was then multiplied by two to account for the gill filaments from the other side of the body.

Gill filaments from the third gill arch were found to be most representative of average filament length, and thus, the medial filament of each bin on the anterior and posterior hemibranchs of this arch was sampled for measures of lamellar frequency and lamellar bilateral surface area. For lamellar frequency, digital images were acquired of the base, middle, and tip of each sampled filament using a camera mounted on a dissection microscope. For lamellar bilateral area, individual lamellae were dissected from the base, middle, and tip of the filaments, mounted on slides, and photographed. Filament and lamellar images were analyzed using NIH Image J computer software.

Gill Microstructure

Gill tissue fixed in 10% formalin was examined using both light microscopy and SEM. For light microscope preparation, fixed tissue was embedded in paraffin, and semithin sections (5 μm) were mounted on slides and stained with hematoxylin and eosin. For SEM, fixed tissue was rinsed with deionized water, slowly dehydrated to 100% ethanol (20–25% increments over 24 h), and critical-point dried. Other sections of fixed gill tissue were rinsed in deionized water, dehydrated with *tert*-butyl alcohol (25% increments over 24 h and rinsed twice at 100%), and frozen in the alcohol at 4°C. Frozen samples were then placed into a freeze dryer until all of the alcohol was extracted from the tissue. Both critical-point-dried and freeze-dried tissues were sputter coated with gold–palladium and viewed using an FEI Quanta 600 SEM under high-vacuum mode. Because criti-

cal-point drying can cause slight shrinkage to gill tissue, cross sections through freeze-dried lamellae were used to estimate lamellar thickness and the water–blood barrier thickness. These measurements were made for eight makos and four blue sharks by randomly sampling filaments from the second, third, and fourth gill arches. Longitudinal cross sections of the freeze-dried filaments were mounted perpendicular to the SEM field of view, and 15 measurements of the two different dimensions were made for each shark.

Gill tissue fixed in paraformaldehyde was used to determine the distribution of mitochondria-rich cells using immunohistochemical methods of Piermarini et al. (2002) and Hyndman and Evans (2007). Gill tissue was dehydrated in ethanol, embedded in paraffin, and sliced into 7- μm sections mounted on slides and heated at 37°C overnight. Slides were analyzed with monoclonal, anti-chicken $\text{Na}^+ - \text{K}^+$ -ATPase ($\alpha 5$, 1/100), developed by Dr. Douglas Fambrough and obtained from the Developmental Studies Hybridoma Bank under the auspices of the National Institute of Child Health and Human Development of the University of Iowa (Department of Biological Sciences, Iowa City, IA). Immunoreactivity was visualized with 3,3'-diaminobenzidine tetrahydrochloride (Biogenex, San Roman, CA). Other sections of paraformaldehyde-fixed tissue were mounted on slides and histologically stained with Masson's Trichrome (Humason, 1997).

Details of general gill circulation were obtained by viewing macerated vascular casts with the SEM under low-vacuum mode. Mako and blue shark lamellar blood-flow patterns were examined by randomly sampling 15 lamellae from each shark cast. Digital scanning electron micrographs were analyzed with Image J by measuring the angle of blood flow relative to the lamellar long axis midway along the length of each lamella.

Statistical Analysis

Mass-regression equations for gill area and dimensions were determined using least-squares analysis. Lamellar thickness, the water–blood barrier thickness, and the angle of lamellar blood flow are presented as means \pm standard deviation. Significant differences for these measurements between species were determined using a general linear model type analysis of covariance (ANCOVA) with individuals and body mass representing covariates.

RESULTS

Gill Surface Areas and Dimensions

Table 1 shows general agreement in the mass-regression equations for total gill surface area and its constituent dimensions (L_{fil} , n_{lam} , and A_{lam}) determined for five makos in this study and the data of Emery and Szczepanski (1986). Also shown in Table 1 is a comparison of values derived from these equations for a 4.48 kg mako, which is the size of the single specimen examined by Oikawa and Kanda (1997). The smaller gill area reported by these authors results primarily from an underestimation of lamellar bilateral area (Table 1), which they calculated by measuring lamellar length and height and assuming a triangular lamellar shape. Because most mako lamellae are generally rectangular, this underestimates lamellar size by a factor of two.

Lamellar Dimensions and Structure

Table 2 shows lamellar measurements for eight makos and four blue sharks. Mako lamellar thick-

TABLE 1. Regression equations for shortfin mako gill morphometrics in relation to body mass (g)

Source	Gill surface area (cm ²)	Total filament length (cm)	Lamellar frequency (mm ⁻¹)	Lamellar bilateral surface area (mm ²)
Regression equations				
Present study	$y = 35.889x^{0.7834}$	$y = 612.310x^{0.2904}$	$y = 39.185x^{-0.1113}$	$y = 0.00748x^{0.6043}$
Emery and Szczepanski (1986)	$y = 57.544x^{0.7400}$	$y = 676.083x^{0.2800}$	$y = 100.00x^{-0.2000}$	$y = 0.00427x^{0.6600}$
Oikawa and Kanda (1997)	—	—	—	—
Mako at 4480 g				
Present study	26023	7035.6	15.4	1.20
Emery and Szczepanski (1986)	28970	7118.0	18.6	1.10
Oikawa and Kanda (1997)	12040	5953.5	17.2	0.59

ness (mean = $11.38 \pm 1.61 \mu\text{m}$) is significantly less than that of the blue shark ($15.24 \pm 3.41 \mu\text{m}$) (ANCOVA, $P < 0.001$), as is the water–blood barrier thickness (mako, $1.15 \pm 0.22 \mu\text{m}$; blue shark, $1.65 \pm 0.59 \mu\text{m}$) ($P < 0.001$). Immunohistochemical-treated cross sections of the gill filaments (Fig. 1) show that in the mako, mitochondria-rich cells, which are involved in ion and acid–base balance, are primarily only present in the interlamellar filamental epithelium (Fig. 1A). This differs from many other fish species, including the single blue shark specimen examined in this study, in which MRCs are also common in the lamellar epithelium (Fig. 1B). The absence of MRCs in the mako's lamellar epithelium contributes to its thin lamellae and short water–blood barrier distance. Table 2 also shows that lamellar thickness in the mako changes less with body size in comparison to that of the blue shark.

Figure 2 compares the patterns of lamellar blood flow in the shortfin mako (A), the blue shark (B), and two high-energy demand teleosts, the yellowfin tuna, *Thunnus albacares* (C), and the eastern Pacific bonito, *Sarda chiliensis* (D). Common to all four species is the presence of a diagonal flow pattern, which differs from that observed for most fishes where blood flows parallel to and along the

length of the lamellar long axis. However, the degree to which these species are specialized for this pattern varies in terms of blood delivery and collection, the angle of diagonal flow, and the extent to which the diagonal pattern proceeds across the lamellar height. In yellowfin tuna (Fig. 2C), blood leaving the afferent lamellar arteriole enters several outer marginal channels that distribute flow along the lamellar lateral edge from which blood proceeds diagonally at an angle of 45° – 70° relative to the lamellar long axis; efferent blood is collected in an inner marginal channel (Muir and Brown, 1971; Wegner et al., 2010). In the mako (Fig. 2A), two outer marginal channels typically distribute flow to the lamellar lateral edge, and the angle of diagonal flow ($38.4^\circ \pm 6.7^\circ$) is reduced. In addition, diagonal flow only extends across two-thirds to three-fourths of the lamellar height and then turns parallel to the long axis of the lamella; blood, therefore, is not collected by a single inner marginal channel. Both the blue shark (Fig. 2B) and eastern Pacific bonito (Fig. 2D) show patterns similar to that of the mako; however, the angle of diagonal flow in each species (blue shark = $28.1^\circ \pm 7.2^\circ$, bonito = $31.9^\circ \pm 6.7^\circ$) is significantly less than that of the mako (ANCOVA; mako vs. blue, $P < 0.001$; mako vs.

TABLE 2. Lamellar dimensions in the shortfin mako and blue shark (means \pm standard deviation)

Species	Mass (kg)	Fork length (cm)	Lamellar thickness (μm)	Water–blood barrier thickness (μm)
Shortfin mako	4.6	77.0	11.26 ± 0.93	1.02 ± 0.13
Shortfin mako	8.3	94.0	10.72 ± 1.33	1.03 ± 0.14
Shortfin mako	10.5	101.5	10.34 ± 1.55	1.10 ± 0.20
Shortfin mako	16.2	116.5	11.97 ± 1.86	1.16 ± 0.20
Shortfin mako	34.0	134.0	11.39 ± 1.39	1.35 ± 0.31
Shortfin mako	49.0	160.5	10.51 ± 0.88	1.23 ± 0.23
Shortfin mako	55.5	167.0	12.27 ± 1.79	1.16 ± 0.16
Shortfin mako	71.0	187.5	12.58 ± 1.57	1.14 ± 0.20
\bar{x}			11.38 ± 1.61	1.15 ± 0.22
Blue shark	2.4	72.0	12.72 ± 1.90	1.44 ± 0.69
Blue shark	3.4	84.0	13.39 ± 2.05	1.23 ± 0.23
Blue shark	44.0	197.0	18.78 ± 3.20	2.07 ± 0.59
Blue shark	47.9	196.0	16.06 ± 2.55	1.88 ± 0.35
\bar{x}			15.24 ± 3.41	1.65 ± 0.59

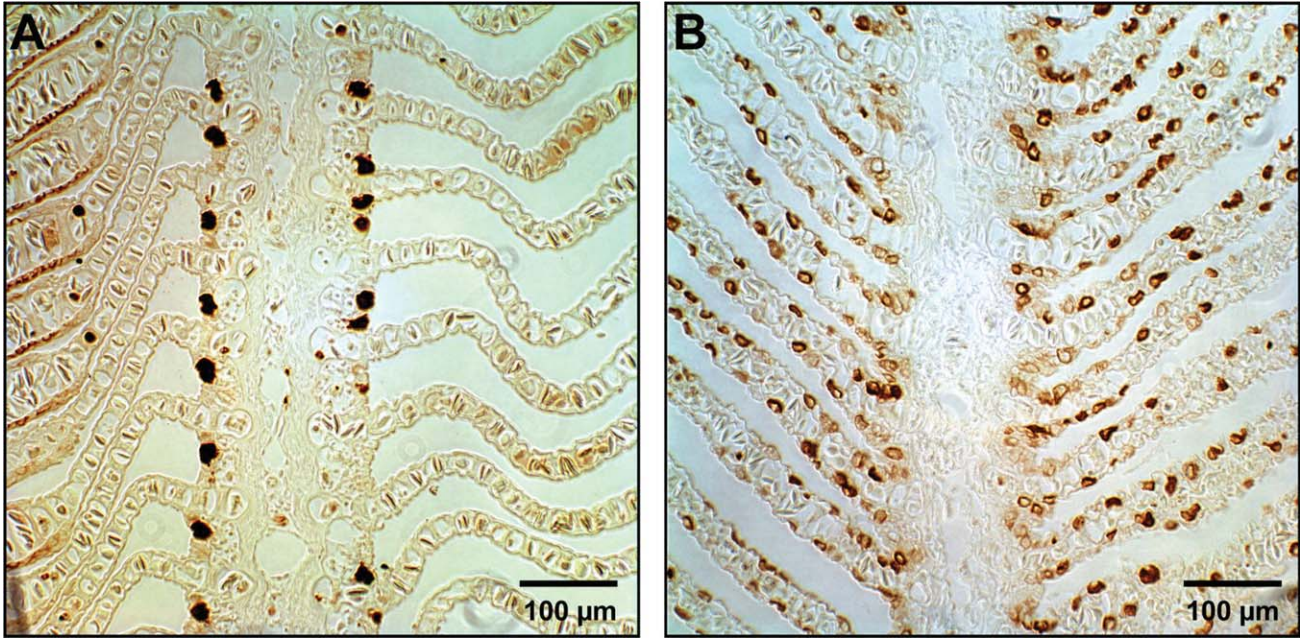


Fig. 1. Longitudinal cross sections through the gill filament of (A) a 24.0 kg shortfin mako and (B) a 44.0 kg blue shark showing the distribution of mitochondria-rich cells (brown).

bonito using raw data from Wegner et al., 2010, $P < 0.01$). In the blue shark, a second outer marginal channel is often absent and, when present, is less developed.

Examination of mako and blue shark lamellae also reveals the presence of previously undescribed

vascular “sacs” near the leading (water-entry, blood-efferent) edges of the lamellae (shown for the mako in Fig. 3). For both species, one to two vascular sacs are present on each lamella (Fig. 3A), and their number generally correlates with lamellar height; lamellae near the filament

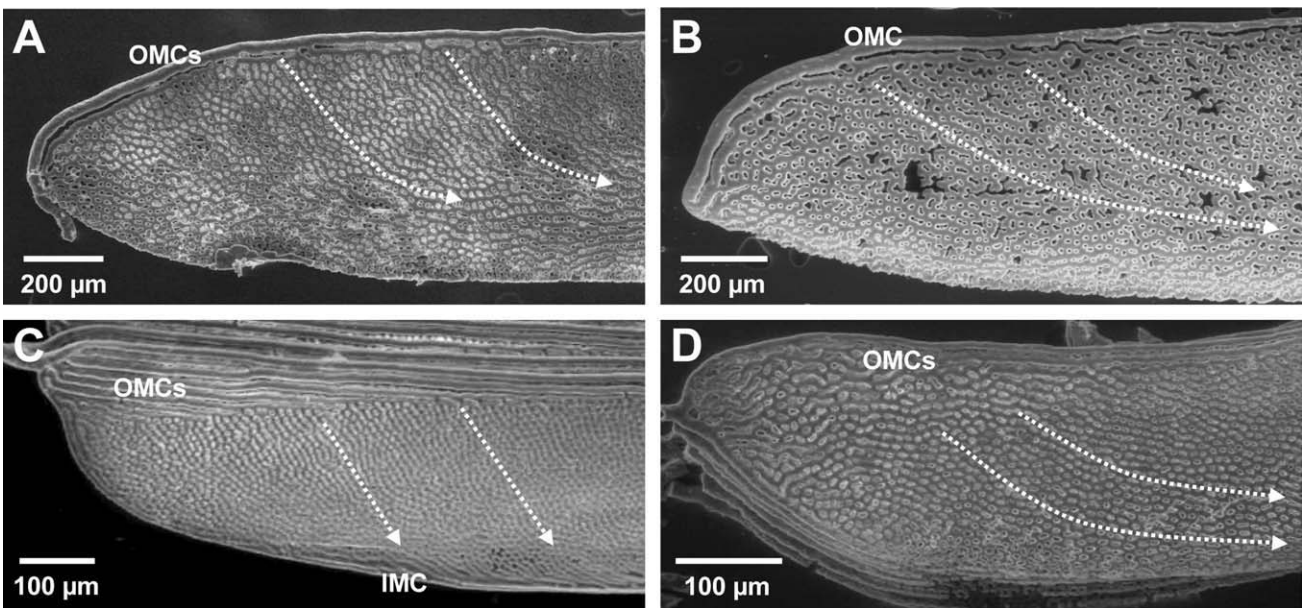


Fig. 2. Scanning electron microscope images of lamellar casts in (A) a 21.2 kg shortfin mako and (B) a 17.1 kg blue shark showing the lamellar vascular channels and the depressions where pillar cells were located. Shown for comparison are cast lamellae from (C) a 4.2 kg yellowfin tuna and (D) a 1.87 kg eastern Pacific bonito (Wegner et al., 2010). Blood flow is indicated by dotted arrows. Water flow is from right to left in all images. IMC, inner marginal channel; OMC, outer marginal channel.

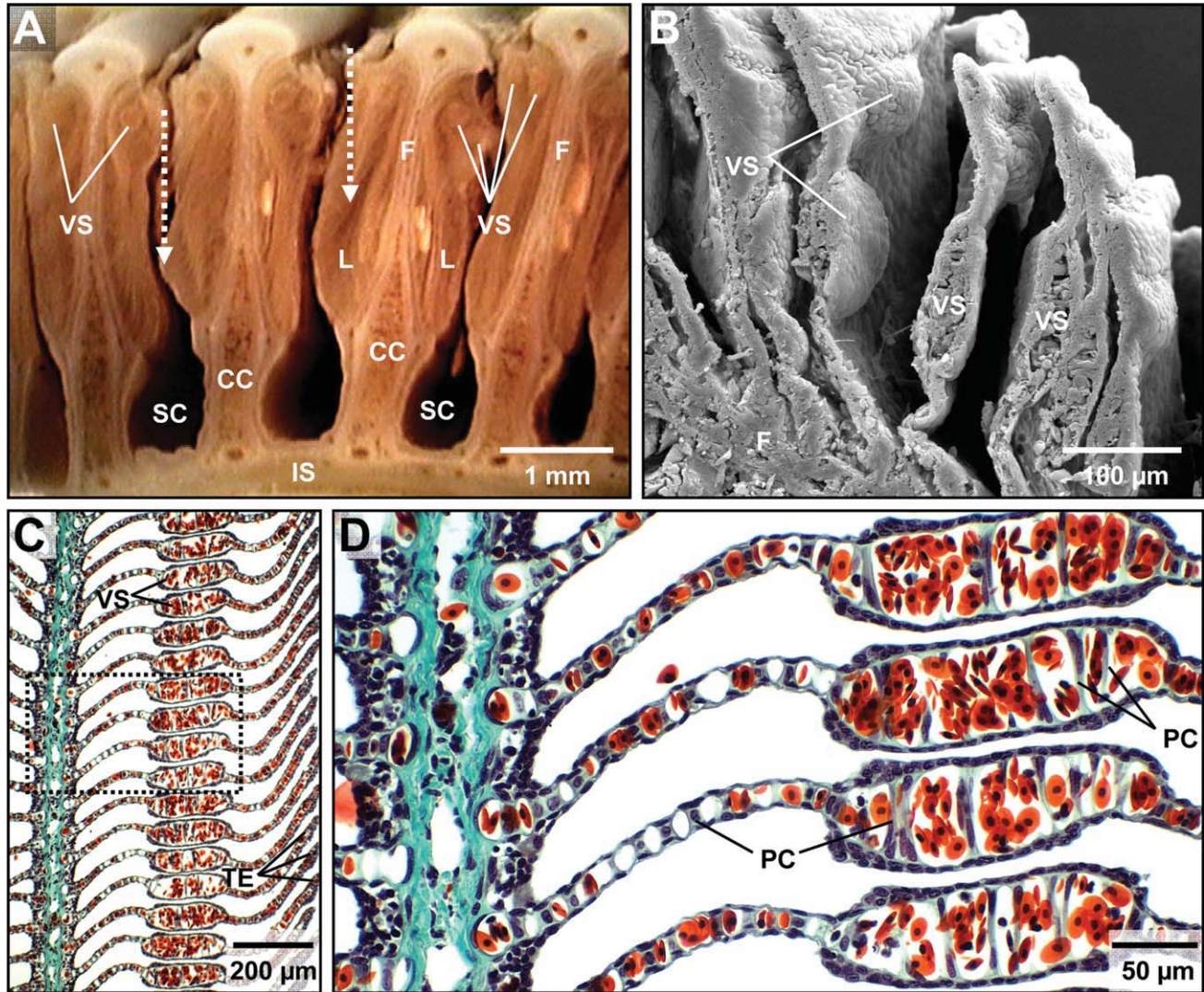


Fig. 3. Images of the lamellar vascular sacs in the shortfin mako. (A) Four adjacent filaments from a 9.0 kg mako showing 1–2 vascular sacs on each lamella near the leading (water-entry) edge. Water flow is indicated by dotted arrows. (B) Scanning electron microscope image of a longitudinal section through the gill filament of a 8.3 kg mako showing the lamellae and vascular sacs. (C) Longitudinal section through a filament of a 9.0 kg mako showing the proximity of vascular sacs between adjacent lamellae and a thick epithelium near the outer marginal edge. (D) Magnified image of dotted box in C showing the details of the vascular sacs filled with red blood cells and supported by large pillar cells. Water flow is into the page in B–D. CC, corpus cavernosum; F, filament; IS, interbranchial septum; L, lamella; PC, pillar cell; SC, septal channel; TE, thick epithelium; VS, vascular sac.

base or associated with shorter filaments have a lower profile and tend to possess only one vascular sac. On taller lamellae, near the middle or tip of the filaments, two vascular sacs are often present. The location of the vascular sacs on each lamella is consistent in that sacs from adjacent lamellae abut one another (Fig. 3B–D) suggesting a function in lamellar stability and spacing. In addition, the efferent lateral edges of mako and blue shark lamellae are covered by a thicker epithelium than that of the lamellar respiratory surface (Fig. 3C), and this may further help stabilize the lamellae. No quantifiable differences in either of these features were found between the mako and blue shark.

Gill Vasculature

The general architecture of the mako gill vasculature is consistent with that of other elasmobranchs. Figure 4 shows the basic features of the gill filament circulation in the mako, which consists of three distinct vascular pathways: respiratory, nutrient, and interlamellar. Blood enters the respiratory vasculature via the afferent filamental artery (AFA), which distributes blood along the length of the filament to the corpus cavernosum (CC; Fig. 4A–D). Afferent lamellar arterioles (ALA) rise from the corpus cavernosum to supply blood to the gill lamellae (Fig. 4E); postlamellar blood flow is collected in efferent lamellar arterioles (ELA),

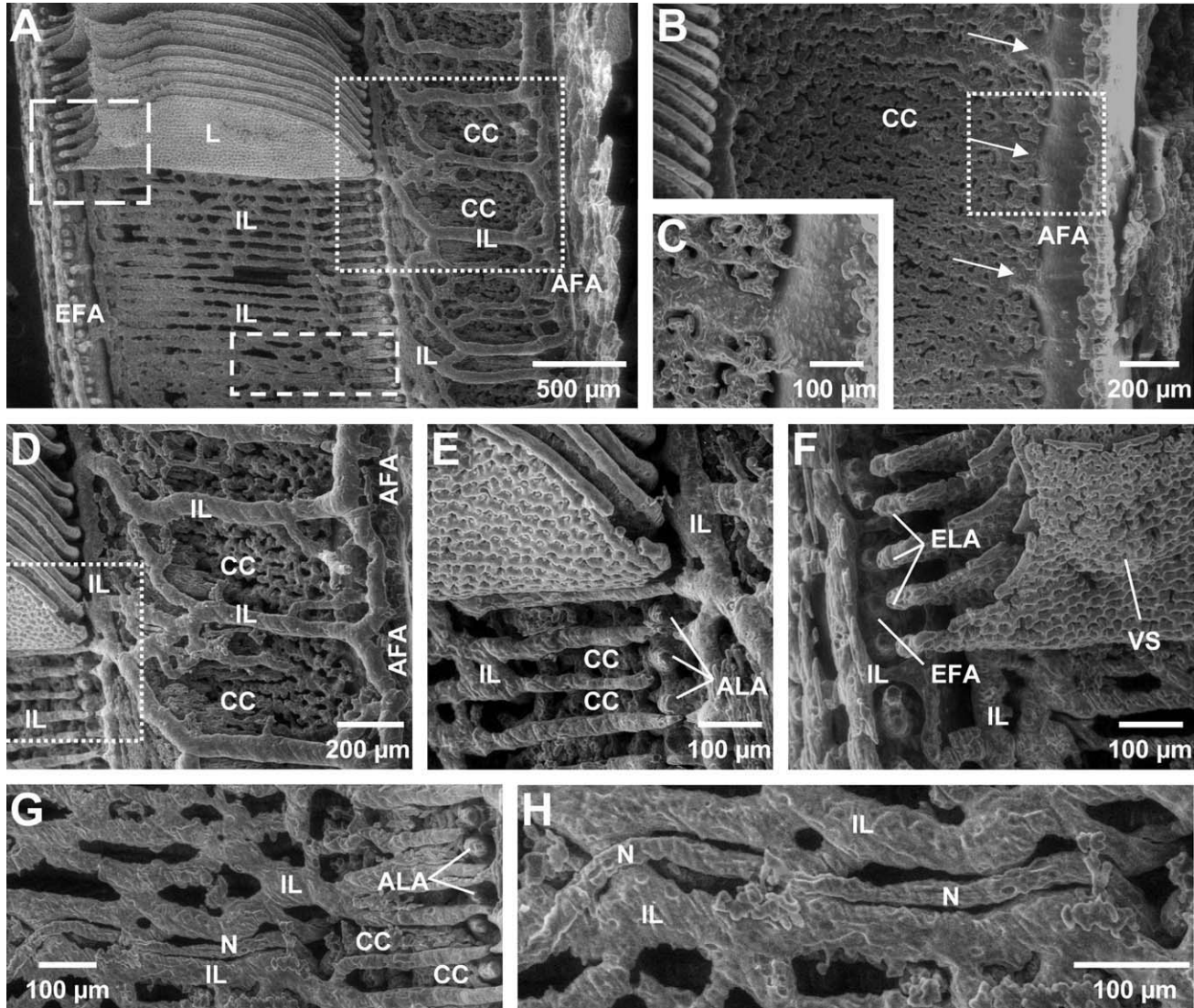


Fig. 4. Scanning electron microscope images of vascular casts from a 5.0 kg shortfin mako showing the general features of the gill filament circulation. (A) Synoptic view of a gill filament. (B) Magnified image of dotted box in A (upper right) with the interlamellar circulation removed to show the corpus cavernosum. Major connections of the corpus cavernosum to the afferent filamentary artery are shown by arrows. (C) Enlarged image of box in B showing connections of the afferent filamentary artery with the corpus cavernosum. (D) Enlarged image of dotted box in A (upper right) with the interlamellar circulation still intact. (E) Magnified image of dotted box in D showing the afferent lamellar arterioles leaving the corpus cavernosum and the interlamellar circulation running underneath the lamellae. (F) Enlarged view of box in A (long dashes, upper left) showing the connection of the efferent lamellar arterioles to the efferent filamentary artery and the cast of a vascular sac on the efferent edge of a lamella. (G) Magnified image of box in A (short dashes, bottom middle) showing a nutrient vessel intertwined with the interlamellar circulation. (H) Enlarged view of G. Water flow is from left to right in all images. AFA, afferent filamentary artery; ALA, afferent lamellar arteriole; CC, corpus cavernosum; EFA, efferent filamentary artery; ELA, efferent lamellar arteriole; L, lamella; IL, interlamellar vessel; N, nutrient vessel; VS, vascular sac.

which feed into an efferent filamentary artery (EFA; Fig. 4F). Gill nutrient vessels (Fig. 4G,H) originate from EFAs and efferent branchial arteries (not shown) and extend throughout the filaments and interbranchial septum. The interlamellar vessels (Fig. 4A, D–H) usually lay perpendicular to the long axis of the filament and extend underneath the interlamellar epithelium, over the corpus cavernosum, and beneath the epithelium lining the septal channel where they connect with the inter-

lamellar vessels of the adjacent filament. The interlamellar vasculature appears to be connected to the main blood supply through anastomoses with small nutrient vessels.

DISCUSSION

Gill Structure and Gas Exchange

Gill structure and function strongly correlate with activity and metabolic demand; active fishes

TABLE 3. Gill dimensions of the shortfin mako in comparison to other elasmobranchs and some high-energy demand teleosts determined by mass-regression equations for a body mass of 10 kg

Species	Gill surface area (cm ²)	Total filament length (cm)	Lamellar frequency (mm ⁻¹)	Lamellar bilateral surface area (mm ²)	Mean lamellar thickness (μm)	Interlamellar spacing (μm)
Shortfin mako ^a	48816	8883.2	14.06	1.95	11.38	59.75
Shortfin mako ^b	52481	8912.5	15.85	1.86	—	—
White shark ^b	51286	13803.8	13.80	1.35	—	—
Blue shark ^b	18212	5370.3	11.22	1.51	15.24	73.88
Dusky shark ^b	20418	7413.1	15.49	0.98	—	—
Skipjack tuna ^c	130588	20027.2	29.34	1.11	—	—
Bluefin-yellowfin tuna ^c	99460	18850.5	26.74	0.98	5.88	31.51
Eastern Pacific bonito ^d	64082	12741.5	31.11	0.81	—	—
Striped marlin ^d	40778	20549.1	22.64	0.44	6.29	37.89

Sources:

^aPresent study.

^bEmery and Szczepanski (1986).

^cMuir and Hughes (1969).

^dWegner et al. (2010).

Mean lamellar thicknesses are not from regression equations; mako and blue shark data are from Table 2, yellowfin tuna and striped marlin measurements are from Wegner et al. (2006). Interlamellar spacing is calculated from lamellar frequency and thickness data.

typically have larger gill surface areas and shorter diffusion distances than species with lower aerobic requirements (Gray, 1954; Hughes, 1966, 1970; Hughes and Morgan, 1973; De Jager and Dekkers, 1975; Wegner et al., 2010). This study of the gill structure of the shortfin mako further confirms this correlation and supports the conclusions of Emery and Szczepanski (1986) that lamnid gill surface areas are 2–3 times larger than those of other sharks (Table 3). Also correlating with activity is the mako's lamellar thickness (11.38 μm) and its water–blood barrier thickness (1.15 μm), both of which are significantly less than those of the blue shark (15.24 and 1.65 μm). The water–blood barrier thicknesses measured for both the mako and the blue shark are far less than the mean distances (4.85–11.27 μm) reported for four less-active, benthic elasmobranch genera (*Scyliorhinus*, *Squalus*, *Galeorhinus*, and *Raja*; Hughes and Wright, 1970).

The mako and blue shark also have a diagonal blood-flow pattern through the gill lamellae, which had previously only been documented for a few high-energy demand teleosts. This pattern differs from that of most fishes in which the course of blood flow through a lamella extends along its entire length, parallel to the lamellar long axis. Although it somewhat compromises the counter-current exchange mechanism, diagonal lamellar blood flow is considered to be an adaptation that optimizes the relationship between the residence time red blood cells spend in lamellar vessels and the time required for oxygen diffusion and loading by hemoglobin (Muir and Brown, 1971; Olson et al., 2003; Wegner et al., 2006; Wegner et al., 2010). Because gas transfer in these fishes is augmented by shorter diffusion distances, the residence time needed for oxygenation becomes less than the time required for blood to move through a vessel parallel to and the length of the lamellar

long axis. Diagonal flow through more numerous shorter channels should contribute to exchange efficacy by closely matching blood residence time to the time constants for the movement and binding of enough oxygen to saturate hemoglobin.

An additional advantage imparted by diagonal flow is a reduction in vascular resistance. This effect is illustrated by the Hagen-Poiseuille equation describing the effects of lamellar-vessel length and diameter on blood pressure drop (Δp) occurring across a lamella:

$$\Delta p = 32\mu Ul/d^2 (\text{Pa}),$$

where μ is the dynamic viscosity, U is the mean velocity of blood flow, l is vessel length, and d is vessel diameter (Muir and Brown, 1971). Under conditions of laminar flow, vascular resistance is minimized by either increasing vessel diameter or decreasing its length. Because vessel diameter in active fishes is constrained by requirements to minimize diffusion distances, a decrease in vessel length, achieved by diagonal flow, is used to minimize the translamellar vascular pressure gradient. The diagonal flow pattern also increases the number of lamellar blood channels in parallel, which further conserves vascular pressure through the gills and helps minimize blood channel diameter and consequently lamellar thickness.

The diagonal blood-flow pattern seen in mako lamellae suggests selection for the optimization of gas transfer efficacy and the conservation of vascular pressure. However, because the mako diagonal flow angle is $38.4^\circ \pm 6.7^\circ$, the relative advantages would be less than those realized by the higher angles of tunas at 45° – 70° (Muir and Brown, 1971; Wegner et al., 2010), which with a thinner water–blood barrier [0.5–0.6 μm in tunas (Hughes, 1970; Wegner et al., 2006), 1.15 μm for the mako] can

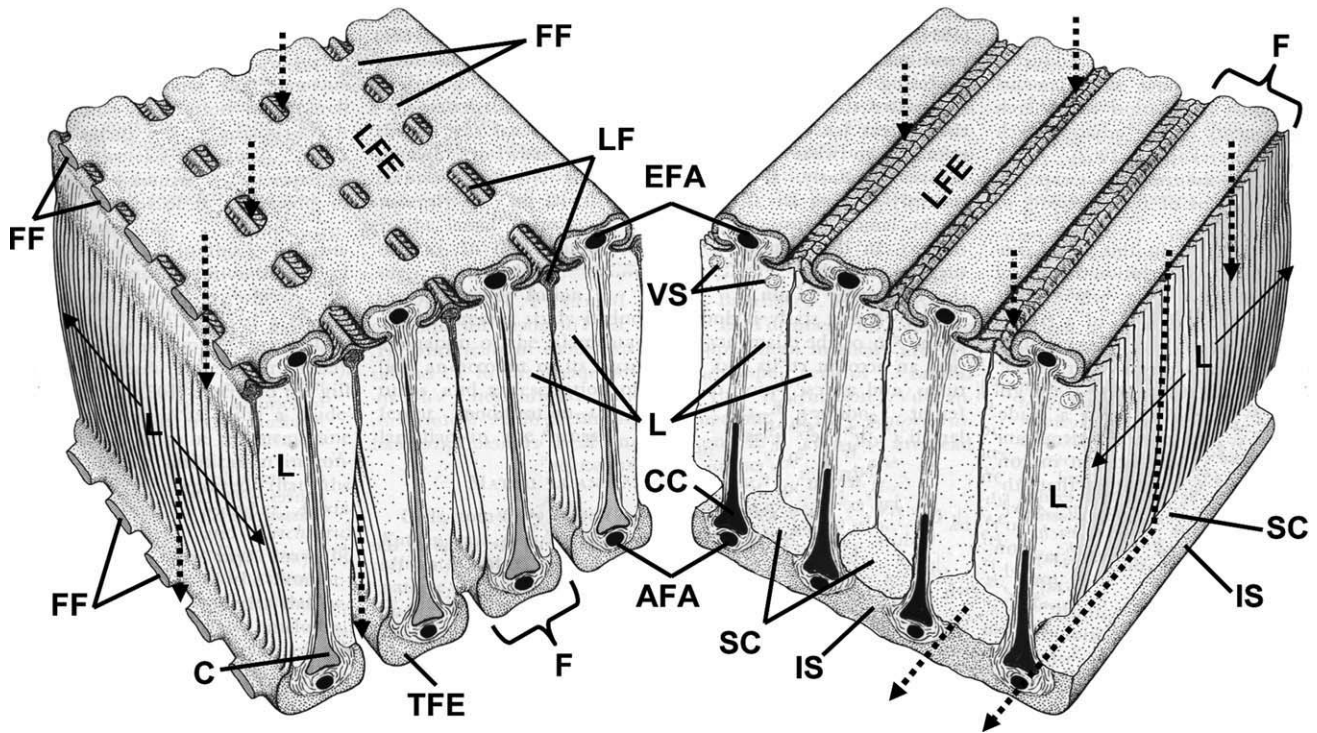


Fig. 5. Comparison of the basic gill features in a tuna (left) and a shortfin mako (right). Dotted arrows indicate water flow direction. AFA, afferent filamental artery; C, cartilaginous filament rod; CC, corpus cavernosum; EFA, efferent filamental artery; F, filament; FF, filament fusion; IS, interbranchial septum; L, lamella; LF, lamellar fusion; LFE, leading filament edge; SC, septal channel; TFE, trailing filament edge; VS, vascular sac. Tuna gill schematic is modified from Muir and Kendall (1968) and Wegner et al. (2006).

potentially optimize gas transfer in shorter vessels. General support for the idea of a graded capacity to optimize oxygenation and vascular resistance is further suggested by the blue shark, which has a diagonal flow angle of $28.1^\circ \pm 7.2^\circ$ and a correspondingly thicker water–blood barrier ($1.65 \mu\text{m}$) than the mako. The reduced angle of blue shark lamellar blood flow also correlates with fewer, longer, and wider blood vessels, which result in thicker lamellae. Moreover, data in Table 2 show less change in mako lamellar thickness with body size in comparison to blue sharks. This suggests that the greater angle of mako diagonal flow helps to conserve lamellar thickness and short diffusion distances with growth.

Gill Structure and Ram Ventilation

In ram-ventilating fishes, the gills must be sufficiently rigid to maintain structural integrity and orientation to continue efficient gas exchange while utilizing the forceful branchial stream produced by fast, continuous swimming. Figure 5 compares the basic gill design features of the shortfin mako and tunas. The elasmobranch interbranchial septum, an extension of the gill arch that attaches to and supports the trailing edges of the gill filaments as it extends laterally outward to form the gill flap, has been suggested as an

important structural feature contributing to gill reinforcement for ram ventilation (Benz, 1984). Teleosts lack this septum and, because the greater part of each gill filament extends without support into the downstream flow, tunas and other rapidly swimming, ram-ventilating teleosts have developed wide, cartilaginous (or in some cases ossified) filament rods (Iwai and Nakamura, 1964) and fusions, which bind the gill filaments and lamellae (see Fig. 5; Muir and Kendall, 1968; Johnson, 1986; Wegner et al., 2006). Because the full length of each elasmobranch filament is connected to the interbranchial septum, this structure lessens the requirement for additional support for ram ventilation, and, even though the septal structure likely adds considerable resistance to branchial flow, selection for this ventilation mode and for continuous swimming in the mako and other lamnids appears to have taken place within this morphological framework.

Other components important in elasmobranch gill support are closely linked to cardiovascular function. The corpus cavernosum, which is in series with the respiratory circulation (see Fig. 4), is thought to function as a hydrostatic skeleton for the gill filament (see Fig. 5; Cooke, 1980; De Vries and De Jager, 1984; Butler, 1999). However, despite the shortfin mako's dependence on ram ventilation, the size and position of the corpus

cavernosum does not appear to differ from that of some less active elasmobranchs (Cooke, 1980; Olson and Kent, 1980). This study documents a second vascular feature that appears important for gill support: previously undescribed vascular “sacs” near the water entry edge of lamellae in both the shortfin mako and blue shark (see Figs. 3 and 5). These sacs appear quite similar to the “button-like epithelial outgrowths” described for the spiny dogfish, *Squalus acanthias*, by De Vries and De Jager (1984), who suggested these structures function to keep the interlamellar spaces open. However, rather than epithelial, the spacers of the mako and blue shark are vascular and are thus likely subject to vasoactive agents and alterations in cardiac output and branchial perfusion.

The connection of both the corpora cavernosa and lamellar sacs to the respiratory circulation suggests the operation of a vascular, pressure-based mechanism (subject to vasoactive control) for maintaining both filament and lamellar structural integrity. For example, an increase in cardiac output associated with exercise would raise ventral aortic pressure, likely stiffening the corpora cavernosa and potentially distending the vascular sacs, thus enhancing both filament and lamellar rigidity during the increased ram-ventilatory flow. Because vascular sacs are located near the water entry edge of each lamella, changes in their size could also affect both the volume and velocity of water through the interlamellar channels. In addition to changes in cardiac output, catecholamines, which are stored in and released from large central venous sinuses in sharks, readily affect heart activity and gill perfusion (Opdyke et al., 1982; Randall and Perry, 1992; Olson and Farrell, 2006) and could serve to further modulate such a mechanism. Also, the recent finding of endothelin (ET_A and ET_B) receptors on the lamellar pillar cells of many fishes, including some elasmobranchs (Evans and Gunderson, 1999; Stensløkken et al., 2006; Hyndman and Evans, 2007), implicates their role in regulating branchial perfusion.

A structural feature that might function in conjunction with vascular regulation is suggested by Figure 3C, which shows that the leading lateral edges of mako lamellae have a much thicker epithelium than that of the gas-exchanging region. This thickening, which was also observed for the blue shark, resembles that described in the wahoo, *Acanthocybium solandri*, a ram-ventilating teleost (Wegner et al., 2006), and, in combination with the lamellar sacs, should contribute to an overall bracing of the lamellae for ram ventilation.

Mako Gills and Upper Limits for the Lamnid-Tuna Convergence

Lamnid sharks and tunas show a remarkable evolutionary convergence in specializations for

locomotion, kinematics, aerobic muscle position, regional endothermy, oxygen delivery to the musculature, and cardiac physiology (Carey et al., 1971; Bernal et al., 2001; Bernal et al., 2003a,b; Dickson and Graham, 2004; Donley et al., 2004; Shadwick, 2005). Despite this suite of similarities, the aerobic capacity of the mako, although greater than that of other sharks, is less than that of tunas (Graham et al., 1990; Sepulveda et al., 2007). Tuna standard metabolic rate is about twice that of the mako (Brill, 1979, 1987; Dewar and Graham, 1994; Sepulveda et al., 2007), and this is correlated with an approximately twofold greater gill surface area (Table 3). The results of this study suggest that basic design features of the elasmobranch gill (see Fig. 5), combined with other physiological characters, may limit the maximum capacity of lamnid aerobic performance at a lower level than that of tunas.

Comparison of the gill morphometrics (Table 3) recruited by lamnids and tunas to increase gill surface area provides insight into the selective factors affecting and potentially limiting lamnid gill size. The mechanisms underlying the increase in lamnid gill surface area above that of other sharks include a large lamellar bilateral surface area (shortfin mako) and a high total filament length (white shark; Table 3). Dimensional changes of this nature are consistent with those leading to increased gill areas in many other fishes and with theoretical predictions for augmenting area without drastically increasing branchial resistance to water flow (Hughes, 1966). Although tunas also have a relatively high total filament length, their gill area is further increased by a high number of lamellae per length of filament (Table 3). This high lamellar frequency results in narrow interlamellar channels (Table 3) that increase branchial resistance and likely help to slow and streamline ram-ventilatory flow (Wegner et al., 2010). In contrast, resistance to water flow through lamnid gills is likely inherently high because of the forcing of water through the septal channels of the elasmobranch gill, and although this may help slow the ram-ventilatory stream, it likely precludes the recruitment of a high lamellar frequency to augment gill surface area (a high lamellar frequency with narrow interlamellar channels would further increase branchial resistance). Accordingly, the lamellar frequencies in the mako and white shark are not significantly greater than those of some nonlamnid sharks and are half those of tunas and many other high-energy demand teleosts (Table 3).

In addition to having a smaller gill surface area than tunas, the mako has both a greater water–blood barrier thickness and lamellar thickness. The thicker water–blood barrier is likely required to provide structural support to its large lamellae. The greater thickness of mako lamellae [11.38 μm in comparison to 5.88 μm in yellowfin

tuna (Wegner et al., 2006)] correlates with wider blood channels that are required to accommodate the large red blood cells intrinsic to all elasmobranchs. Thus, although mako diffusion distances are shorter than those of the blue shark and other elasmobranchs, they are much greater than those of tunas, and this, in addition to a smaller gill area, may ultimately limit comparable gill function.

SUMMARY

This study demonstrates three morphological features that distinguish mako gills from those of other sharks and that correlate with the mako's relatively higher metabolic demands: 1) a larger gill surface area, 2) shorter lamellar diffusion distances, and 3) a more fully developed diagonal blood-flow pattern through the lamellae. However, in comparison to tunas, the mako gill area is about half the size, the water-blood barrier is twice as thick, and the angle of lamellar diagonal blood flow is reduced. In addition, this study suggests that mako gill structure (despite the discovery of vascular sacs, which appear to enhance lamellar stability) is not more specialized than that of the blue shark in features related to ram ventilation. This differs from the highly modified gills of tunas, which have filament and lamellar fusions to increase gill rigidity and densely packed lamellae that slow and streamline ram-ventilatory flow. The difference in the degree of lamnid gill specialization appears related to inherent structural features of the elasmobranch gill. Although the interbranchial septum increases the structural integrity of the elasmobranch gill and may consequently facilitate ram ventilation, it also increases branchial resistance and may ultimately limit gill surface area. The lower gill area of lamnids parallels findings of previous lamnid-tuna comparisons showing that, despite convergent adaptations increasing the rates of oxygen uptake and delivery, the relative metabolic capacity of lamnids, as determined by factors such as mitochondrial density, enzymatic activities, and oxygen consumption, is less than that of tunas.

ACKNOWLEDGMENTS

The authors thank P. Hastings, M. McHenry, F. Powell, R. Rosenblatt, and two anonymous reviewers for their comments on this manuscript. They also thank S. Aalbers, N. Ben-Aderet, L. Field, D. Kacev, S. Kohin, H. Marshall, M. Musyl, R. Vetter, and the crews of the *David Starr Jordan* and *Oscar Elton Sette* for their help in the collection and preparation of mako and blue shark gill tissue. Additionally, they are grateful to K. Bull and L. Williams for helping with gill area meas-

urements and E. York and B. Neal for technical assistance with microscopy.

LITERATURE CITED

- Altringham JD, Block BA. 1997. Why do tuna maintain elevated slow muscle temperatures? Power output of muscle isolated from endothermic and ectothermic fish. *J Exp Biol* 200:2617–2627.
- Benz GW. 1984. On the conservative nature of the gill filaments of sharks. *Env Biol Fish* 10:111–116.
- Bernal D, Dickson KA, Shadwick RE, Graham JB. 2001. Analysis of the evolutionary convergence for high performance swimming in lamnid sharks and tunas. *Comp Biochem Physiol* 129:695–726.
- Bernal D, Donley JM, Shadwick RE, Syme DA. 2005. Mammal-like muscles power swimming in a cold-water shark. *Nature* 437:1349–1352.
- Bernal D, Sepulveda C, Mathieu-Costello O, Graham JB. 2003a. Comparative studies of high performance swimming in sharks. I. Red muscle morphometrics, vascularization and ultrastructure. *J Exp Biol* 206:2831–2843.
- Bernal D, Smith D, Lopez G, Weitz D, Grimmering T, Dickson K, Graham JB. 2003b. Comparative studies of high performance swimming in sharks. II. Metabolic biochemistry of locomotor and myocardial muscle in endothermic and ectothermic sharks. *J Exp Biol* 206:2845–2857.
- Brill RW. 1979. Effect of body size on the standard metabolic rate of skipjack tuna, *Katsuwonus pelamis*. *Fish Bull* 77:494–498.
- Brill RW. 1987. On the standard metabolic rates of tropical tunas, including the effect of body size and acute temperature change. *Fish Bull* 85:25–36.
- Brill RW, Bushnell PG. 1991. Metabolic and cardiac scope of high-energy demand teleosts, the tunas. *Can J Zool* 69:2002–2009.
- Brill RW, Bushnell PG. 2001. The cardiovascular system of tunas. In: Block BA, Stevens ED, editors. *Tuna: Physiology, Ecology and Evolution*. San Diego: Academic Press. pp 79–120.
- Bushnell PG, Jones DR. 1994. Cardiovascular and respiratory physiology of tuna: Adaptations for support of exceptionally high metabolic rates. *Env Biol Fish* 40:303–318.
- Butler PJ. 1999. Respiratory system. In: Hamlett WC, editor. *Sharks, Skates and Rays: The Biology of Elasmobranch Fishes*. Baltimore: Johns Hopkins University Press. pp 174–197.
- Carey FG, Teal JM. 1966. Heat conservation in tuna fish muscle. *Proc Natl Acad Sci USA* 56:1461–1469.
- Carey FG, Teal JM, Kanwisher JW, Lawson KD, Beckett JS. 1971. Warm-bodied fish. *Am Zool* 11:137–145.
- Cooke IRC. 1980. Functional aspects of the morphology and vascular anatomy of the gills of the endeavour dogfish, *Centropristis striata* (McCulloch) (Elasmobranchii: Squalidae). *Zoomorphologie* 94:167–183.
- De Jager S, Dekkers WJ. 1975. Relations between gill structure and activity in fish. *Neth J Zool* 25:276–308.
- De Vries R, De Jager S. 1984. The gill in the spiny dogfish, *Squalus acanthias*: Respiratory and nonrespiratory function. *Am J Anat* 169:1–29.
- Dewar H, Graham JB. 1994. Studies of tropical tuna swimming performance in a large water tunnel. I. Energetics. *J Exp Biol* 192:13–31.
- Dickson KA, Graham JB. 2004. Evolution and consequences of endothermy in fishes. *Physiol Biochem Zool* 77:998–1018.
- Dickson KA, Gregorio MO, Gruber SJ, Loeffler KL, Tran M, Terrell C. 1993. Biochemical indices of aerobic and anaerobic capacity in muscle tissues of California elasmobranch fishes differing in typical activity level. *Mar Biol* 117:185–193.
- Donley JM, Sepulveda CA, Konstantinidis P, Gemballa S, Shadwick RE. 2004. More than skin deep: Convergent evolution in mechanical design of lamnid sharks and tunas. *Nature* 429:61–65.

- Emery SH. 1986. Hematological comparisons of endothermic vs. ectothermic elasmobranch fishes. *Copeia* 1986:700–705.
- Emery SH, Szczepanski A. 1986. Gill dimensions in pelagic elasmobranch fishes. *Biol Bull* 171:441–449.
- Evans DH, Gunderson MP. 1999. Characterization of an endothelin ET_B receptor in the gill of the dogfish shark *Squalus acanthias*. *J Exp Biol* 202:3605–3610.
- Gemballa S, Konstantinidis P, Donley JM, Sepulveda C, Shadwick RE. 2006. Evolution of high-performance swimming in sharks: Transformations of the musculotendinous system from subcarangiform to thunniform swimmers. *J Morphol* 267:477–493.
- Graham JB, Dickson KA. 2001. Anatomical and physiological specializations for endothermy. In: Block BA, Stevens ED, editors. *Tuna: Physiology, Ecology and Evolution*. San Diego: Academic Press. pp 121–165.
- Graham JB, Dewar H, Lai NC, Lowell WR, Arce SM. 1990. Aspects of shark swimming performance determined using a large water tunnel. *J Exp Biol* 151:175–192.
- Gray IE. 1954. Comparative study of the gill area of marine fishes. *Biol Bull* 107:219–225.
- Hughes GM. 1966. The dimensions of fish gills in relation to their function. *J Exp Biol* 45:177–195.
- Hughes GM. 1970. Morphological measurements on the gills of fishes in relation to their respiratory function. *Folia Morphol* 18:78–95.
- Hughes GM. 1984a. General anatomy of the gills. In: Hoar WS, Randall DJ, editors. *Fish Physiology*. San Diego: Academic Press. pp 1–72.
- Hughes GM. 1984b. Measurement of gill area in fishes: Practices and problems. *J Mar Biol Ass UK* 64:637–655.
- Hughes GM, Wright DE. 1970. A comparative study of the ultrastructure of the water-blood pathway in the secondary lamellae of teleost and elasmobranch fishes—Benthic forms. *Z Zellforsch Microsk Anat* 104:478–493.
- Hughes GM, Morgan M. 1973. The structure of fish gills in relation to their respiratory function. *Biol Rev* 48:419–475.
- Humason GL. 1997. *Humason's Animal and Tissue Techniques*. Baltimore: Johns Hopkins University Press. 597p.
- Hyndman KA, Evans DH. 2007. Endothelin and endothelin converting enzyme-1 in the fish gill: Evolutionary and physiological perspectives. *J Exp Biol* 210:4286–4297.
- Iwai T, Nakamura I. 1964. Branchial skeleton of the bluefin tuna with special reference to the gill rays. *Bull Misaki Mar Biol Inst Kyoto Univ* 6:21–25.
- Johnson GD. 1986. Scombroid phylogeny: An alternative hypothesis. *Bull Mar Sci* 39:1–41.
- Kohler NE, Casey JG, Turner PA. 1995. Length-weight relationships for 13 species of sharks from the western North Atlantic. *Fish Bull* 93:412–418.
- Korsmeyer KE, Dewar H. 2001. Tuna metabolism and energetics. In: Block BA, Stevens ED, editors. *Tuna: Physiology, Ecology and Evolution*. San Diego: Academic Press. pp 35–78.
- Lai NC, Korsmeyer KE, Katz S, Holts DB, Laughlin LM, Graham JB. 1997. Hemodynamics and blood properties of the shortfin mako shark (*Isurus oxyrinchus*). *Copeia* 1997:424–428.
- Muir BS, Kendall JI. 1968. Structural modifications in the gills of tunas and some other oceanic fishes. *Copeia* 1968:388–398.
- Muir BS, Hughes GM. 1969. Gill dimensions for three species of tunny. *J Exp Biol* 51:271–285.
- Muir BS, Brown CE. 1971. Effects of blood pathway on the blood-pressure drop in fish gills, with special reference to tunas. *J Fish Res Bd Can* 28:947–955.
- Oikawa S, Kanda T. 1997. Some features of the gills of a megamouth shark and a shortfin mako, with reference to metabolic activity. In: Yano K, Morrisey JF, Yabumoto Y, Nakaya K, editors. *Biology of the Megamouth Shark*. Tokyo: Tokyo University. pp 93–104.
- Olson KR, Kent B. 1980. The microvasculature of the elasmobranch gill. *Cell Tissue Res* 209:49–63.
- Olson KR, Farrell AP. 2006. The cardiovascular system. In: Evans DH, Claiborne JB, editors. *The Physiology of Fishes*, 3rd ed. Boca Raton: CRC Press. pp 119–152.
- Olson KR, Dewar H, Graham JB, Brill RW. 2003. Vascular anatomy of the gills in a high energy demand teleost, the skipjack tuna (*Katsuwonus pelamis*). *J Exp Zool A* 297:17–31.
- Opdyke DF, Carroll RG, Keller NE. 1982. Catecholamine release and blood pressure changes induced by exercise in dogfish. *Am J Physiol* 242:R306–R310.
- Perry CN, Cartamil DP, Bernal D, Sepulveda CA, Theilmann RJ, Graham JB, Frank LR. 2007. Quantification of red myotomal muscle volume and geometry in the shortfin mako shark (*Isurus oxyrinchus*) and the salmon shark (*Lamna ditropis*) using T-1-weighted magnetic resonance imaging. *J Morphol* 268:284–292.
- Piermarini PM, Verlander JW, Royaux IE, Evans DH. 2002. Pendrin immunoreactivity in the gill epithelium of a euryhaline elasmobranch. *Am J Physiol Regul Integr Comp Physiol* 283:R983–R992.
- Randall DJ, Perry SF. 1992. Catecholamines. In: Hoar WS, Randall DJ, Farrell AP, editors. *Fish Physiology*, Vol. 12B. San Diego: Academic Press. pp 255–300.
- Sepulveda CA, Graham JB, Bernal D. 2007. Aerobic metabolic rates of swimming juvenile mako sharks, *Isurus oxyrinchus*. *Mar Biol* 152:1087–1094.
- Shadwick RE. 2005. How tunas and lamnid sharks swim: An evolutionary convergence. *Am Sci* 93:524–531.
- Stensløkken KO, Sundin L, Nilsson GE. 2006. Endothelin receptors in teleost fishes: Cardiovascular effects and branchial distribution. *Am J Physiol* 290:R852–R860.
- Wegner NC, Sepulveda CA, Graham JB. 2006. Gill specializations in high-performance pelagic teleosts, with reference to striped marlin (*Tetrapturus audax*) and wahoo (*Acanthocybium solandri*). *Bull Mar Sci* 79:747–759.
- Wegner NC, Sepulveda CA, Bull KB, Graham JB. 2010. Gill morphometrics in relation to gas transfer and ram ventilation in high-energy demand teleosts: Scombrids and billfishes. *J Morphol* 271:36–49.